April 14, 2010

A two dimensional analogue of the Luttinger model

Edwin Langmann

Theoretical Physics, KTH
AlbaNova
SE-10691 Stockholm, Sweden
langmann@kth.se

Abstract

We present a fermion model that is, as we suggest, a natural 2D analogue of the Luttinger model. We derive this model as a partial continuum limit of a 2D spinless lattice fermion system with local interactions and away from half filling. In this derivation, we use certain approximations that we motivate by physical arguments. We also present mathematical results that allow an exact treatment of parts of the degrees of freedom of this model by bosonization, and we propose to treat the remaining degrees of freedom by mean field theory.

Keywords: Lattice fermions; quantum field theory in 2+1 dimensions; bosonization
MSC-class: 81Q80; 81T25; 81T27

1 Introduction

Lattice fermion systems in *one* dimension can be studied successfully by various different methods and are by-now well understood. One powerful approach is to perform a particular continuum limit leading to a low-energy effective model which can be solved analytically. This limit amounts to linearizing the 1D tight-binding band relation at the locations of the non-interacting Fermi surface (consisting of two points) and then removing the ultra-violet (UV) cutoff. In the simplest case of spinless lattice fermions with short-range interactions away from half-filling, one thus obtains the Luttinger model [1] which can be solved exactly using bosonization [2]; see [3, 4, 5] for closely related pioneering work. It is worth stressing that exact solubility means a lot in this case: not only the partition function but also all Green's functions of the model can be computed by analytical methods; see e.g. [6] and references therein. This method can be generalized to 1D Hubbard type systems and is the basis of a paradigm for 1D interacting fermion systems [7]; see e.g. [8] for a textbook presentation. We note that bosonization is based on precise mathematical results; see e.g. [9] or [10].

In this paper, we propose a similar approach in two dimensions. Starting from a 2D analogue of the spinless lattice fermion system mentioned above, we propose a particular

partial continuum limit that makes this system amenable to an analytical, non-perturbative treatment in a finite doping regime away from half filling. This limit leads to a model that, as we suggest, is a natural 2D analogue of the Luttinger model. Different from 1D, only parts of the fermion degrees of freedom of this model can be bosonized and thus treated exactly. We propose to treat the remaining degrees of freedom using mean field theory. We also argue that there is a finite doping regime away from half filling at which these remaining degrees of freedom have an energy gap and that in this regime an exactly solvable truncation of the model can be used. Our approach is applicable beyond weak coupling. Previous work on bosonization in 2D [11, 12, 13, 14, 15, 16, 17, 18] is shortly discussed at the end of Section 7.

Our derivation of this 2D analogue of the Luttinger model relies on approximations that we justify by physical arguments; see Section 5. Our proposal that this model gives a low energy effective description of 2D lattice fermions is therefore, from a mathematical point of view, a conjecture. At any rate, this model is mathematically well-defined and can be treated rigorously. To our opinion, it also has a certain mathematical beauty and naturalness; see (31)–(32). The details of our approach are quite involved [19, 20, 21], and the aim of this letter is to concisely present the main ideas and results.

We define our notation and the lattice fermion system that we take as starting point in Section 2. Section 3 gives a summary of our results, including a self-contained definition of the 2D analogue of the Luttinger model. In Section 4, we discuss physical arguments and experiments that motivate and guide our approach. Our derivation of the model and its treatment by bosonization are outlined in Sections 5 and 6, respectively. Section 7 contains final remarks.

2 Two dimensional t-V model

2.1 Notation

We consider a square lattice with $\mathcal{N} \gg 1$ sites and denote fermion momenta as $\mathbf{k}, \mathbf{k}'$. We write $\mathbf{k} = (k_1, k_2) = k_+\mathbf{e}_+ + k_-\mathbf{e}_-$ with $\mathbf{e}_\pm = (1, \pm 1)/\sqrt{2}$, i.e. $k_\pm = (k_1 \pm k_2)/\sqrt{2}$, and similarly for other 2D vectors $\mathbf{p}$ etc. We introduce a lattice constant $a > 0$ so that $-\pi/a \leq k_{1,2} < \pi/a$, and our large distance cut-off L (system size) is such that $k_\pm \in (2\pi/L)(\mathbb{Z}+1/2)$ and $L/a \in 4\sqrt{2}(\mathbb{N}+1/2)$, i.e. $\mathcal{N} = (L/a)^2$. The set of all such $\mathbf{k}$ is denoted as BZ (Brillouin zone). We use the symbol $\mathbf{p}$ for differences of fermion momenta, and $\tilde{\Lambda}^*$ is the set of all $\mathbf{p}$ such that $p_\pm \in (2\pi/L)\mathbb{Z}$. Fermion operators $\hat{\psi}(\mathbf{k})$ are defined for $\mathbf{k} \in$ BZ and normalized such that $\{\hat{\psi}(\mathbf{k}), \hat{\psi}^\dagger(\mathbf{k}')\} = \delta_{\mathbf{k},\mathbf{k}'}[L/(2\pi)]^2$, and we use the same normalization for other fermion operators $\hat{\psi}_{r,s}(\mathbf{k})$ introduced in Section 3. We write $\hat{\psi}^\dagger\hat{\psi}(\mathbf{k})$ short for $\hat{\psi}^\dagger(\mathbf{k})\hat{\psi}(\mathbf{k})$ etc. We use the abbreviations $\tilde{a} = 2\sqrt{2}a$. The symbol δ_a denotes the lattice periodic Kronecker delta, i.e. $\delta_a(\mathbf{p}) = 1$ if $\mathbf{p} \in (2\pi/a)\mathbb{Z}^2$ and 0 otherwise. Finally, $[\mathbf{k}+\mathbf{k}']$ is the sum of two momenta in BZ modulo $(2\pi/a)\mathbb{Z}^2$, i.e. it is equal to $\mathbf{k} + \mathbf{k}' + (2\pi/a)\mathbf{n} \in$ BZ with appropriate $\mathbf{n} \in \mathbb{Z}^2$.

2.2 Definitions

The lattice fermion model we consider is the so-called 2D t-V model. It describes spinless fermions on a 2D square lattice with $\mathcal{N}$ sites and hopping and repulsive density-density interactions between nearest neighbor sites. It is defined by the Hamiltonian

$$H_{tV} = H_0 - \mu N + H_{\text{int}} \tag{1}$$

with the free part

$$H_0 = \left(\tfrac{2\pi}{L}\right)^2 \sum_{\mathbf{k}\in \text{BZ}} \epsilon(\mathbf{k})\, \hat{\psi}^\dagger \hat{\psi}(\mathbf{k}) \tag{2}$$

and $\epsilon(\mathbf{k}) = -2t[\cos(ak_1) + \cos(ak_2)]$ the tight binding band relation,

$$N = \left(\tfrac{2\pi}{L}\right)^2 \sum_{\mathbf{k}\in \text{BZ}} \hat{\psi}^\dagger \hat{\psi}(\mathbf{k}) \tag{3}$$

the fermion number operator, and $\mu \in \mathbb{R}$ the chemical potential. The interaction is

$$H_{\text{int}} = \left(\tfrac{2\pi}{L}\right)^6 \sum_{\mathbf{k}_j\in \text{BZ}} \hat{\psi}^\dagger(\mathbf{k}_1)\hat{\psi}(\mathbf{k}_2)\hat{\psi}^\dagger(\mathbf{k}_3)\hat{\psi}(\mathbf{k}_4)\hat{u}(\mathbf{k}_1-\mathbf{k}_2)\delta_a(\mathbf{k}_1-\mathbf{k}_2+\mathbf{k}_3-\mathbf{k}_4) \tag{4}$$

with $\hat{u}(\mathbf{p}) = a^2 V[\cos(ap_1) + \cos(ap_2)]/(8\pi^2)$ the Fourier transform of a nearest neighbor interaction. The model parameters t (hopping constant) and V (coupling strength) both are positive. The *filling parameter* is defined as

$$\nu = \frac{\langle N \rangle}{\mathcal{N}} \tag{5}$$

where $\langle\cdot\rangle$ denotes the ground state expectation value. It is in the range $0 \le \nu \le 1$ with half filling corresponding to $\nu = 1/2$, and $\nu - 1/2$ is referred to as doping.

The Hamiltonian H_{tV} is invariant under the particle-hole transformation

$$\hat{\psi}(\mathbf{k}) \to \hat{\psi}^\dagger(\mathbf{k} + \mathbf{Q}/a), \quad \mu \to V - \mu, \quad \nu \to 1 - \nu \tag{6}$$

for $\mathbf{Q} = (\pi, \pi)$, up to an irrelevant additive constant. We therefore can restrict ourselves to $\nu \ge 1/2$.

3 Summary of results

The 2D analogue of the Luttinger model describes six flavors of fermions $\hat{\psi}_{r,s}(\mathbf{k})$ with flavor indices $r = \pm$ and $s = 0, \pm$ and momenta $\mathbf{k}$ in different Fourier spaces Λ_s^* as follows,

$$\begin{aligned} \Lambda_0^* &= \left\{ \mathbf{k} \,|\, k_\pm \in \tfrac{2\pi}{L}(\mathbb{Z} + \tfrac{1}{2}),\ -\frac{\pi}{\tilde{a}} \le k_\pm < \frac{\pi}{\tilde{a}} \right\} \\ \Lambda_{s=\pm}^* &= \left\{ \mathbf{k} \,|\, k_\pm \in \tfrac{2\pi}{L}(\mathbb{Z} + \tfrac{1}{2}),\ -\infty < k_s < \infty,\ -\frac{\pi}{\tilde{a}} \le k_{-s} < \frac{\pi}{\tilde{a}} \right\}. \end{aligned} \tag{7}$$

We refer to the fermions with $s = 0$ and $s = \pm$ as *nodal* and *antinodal*, respectively. The Hamiltonian defining this model is

$$H = H_n + H_a \tag{8}$$

with the nodal part

$$\begin{aligned} H_n = &\sum_{s=\pm}\Big(\big(\tfrac{2\pi}{L}\big)^2 \sum_{\mathbf{k}\in\Lambda_s^*}\sum_{r=\pm} r v_F k_s :\hat{\psi}^\dagger_{r,s}\hat{\psi}_{r,s}(\mathbf{k}): + \\ &\big(\tfrac{1}{L}\big)^2 \sum_{\mathbf{p}\in\tilde{\Lambda}^*}\chi(\mathbf{p})\big[g_1\sum_{r=\pm}\hat{J}^\dagger_{r,s}\hat{J}_{-r,s}(\mathbf{p}) + g_2\sum_{r,r'=\pm}\hat{J}^\dagger_{r,s}\hat{J}_{r',-s}(\mathbf{p})\big]\Big) \end{aligned} \tag{9}$$

and the antinodal part (including nodal-antinodal interactions)

$$\begin{aligned} H_a = &\big(\tfrac{2\pi}{L}\big)^2 \sum_{\mathbf{k}\in\Lambda_0^*}\sum_{r=\pm}(-rc_F k_+k_- - \mu_a) :\hat{\psi}^\dagger_{r,0}\hat{\psi}_{r,0}(\mathbf{k}): + \\ &\big(\tfrac{1}{L}\big)^2 \sum_{\mathbf{p}\in\tilde{\Lambda}^*}\big[g_3\sum_{r=\pm}\hat{J}^\dagger_{r,0}\hat{J}_{-r,0}(\mathbf{p}) + g_4\sum_{r,r',s=\pm}\chi(\mathbf{p})\hat{J}^\dagger_{r,0}\hat{J}_{r',s}(\mathbf{p})\big] \end{aligned} \tag{10}$$

(the model parameters v_F, c_F, g_j, and μ_a are specified further below). The $\hat{J}_{r,s}$ are Fourier transformed and normal ordered fermion densities defined as follows,

$$\begin{aligned} \hat{J}_{r,0}(\mathbf{p}) &= \big(\tfrac{2\pi}{L}\big)^2 \sum_{\mathbf{k}\in\Lambda_0^*} :\hat{\psi}^\dagger_{r,0}(\mathbf{k}-\mathbf{p})\hat{\psi}_{r,0}(\mathbf{k}): \\ \hat{J}_{r,s=\pm}(\mathbf{p}) &= \big(\tfrac{2\pi}{L}\big)^2 \sum_{\mathbf{k}\in\Lambda_s^*}\sum_{n\in\mathbb{Z}} :\hat{\psi}^\dagger_{r,s}(\mathbf{k}-\mathbf{p})\hat{\psi}_{r,s}(\mathbf{k}+2\pi n\mathbf{e}_{-s}/\tilde{a}): \end{aligned} \tag{11}$$

and $\hat{J}^\dagger_{r,s}\hat{J}_{r',s'}(\mathbf{p})$ is short for $\hat{J}_{r,s}(-\mathbf{p})\hat{J}_{r',s'}(\mathbf{p})$. We also use the cutoff functions

$$\chi(\mathbf{p}) = 1 \text{ if } -\pi/\tilde{a} \le p_\pm \le \pi/\tilde{a} \text{ and } 0 \text{ otherwise.} \tag{12}$$

The colons indicate normal ordering with respect to a non-interacting groundstate Ω defined by the conditions

$$\hat{\psi}_{r,\pm}(\mathbf{k})\Omega = \hat{\psi}^\dagger_{r,\pm}(-\mathbf{k})\Omega = 0 \;\text{ if } rk_\pm > 0 \tag{13}$$

and $\hat{\psi}^\dagger_{r,0}(\mathbf{k})\Omega = 0$ or $\hat{\psi}_{r,0}(\mathbf{k})\Omega = 0$ if $rk_+k_- > 0$ or < 0, respectively. In the theorem below we set $\hat{J}_{r,s=\pm}(\mathbf{p}) = 0$ for $|p_{-s}| > \pi/\tilde{a}$.

We first outline how the model above can be derived from the 2D t-V model using certain approximations (Section 5). This allows us to determine the model parameters as follows,

$$c_F = 2ta^2, \quad v_F = 2\sqrt{2}ta\sin(Q), \quad Q = \pi\nu \tag{14}$$

$$g_1 = 2g_2 = 2V\sin^2(Q)a^2, \quad g_3 = g_4 = 2Va^2 \tag{15}$$

$$\mu_a = -\left(4t + \frac{V}{4}\right)\cos(Q) + V\cos^2(Q)\left(1 - \frac{2Q}{\pi}\right) \tag{16}$$

with $0 < |\nu - 1/2| < 1/4$. The key result to bosonize the model above is the following.

Theorem: *(a) The nodal density operators obey the relations*

$$[\hat{J}_{r,s}(\mathbf{p}), \hat{J}_{r',s'}(\mathbf{p}')] = \delta_{r,r'}\delta_{s,s'}\frac{2\pi p_s}{\tilde{a}}\delta_{\mathbf{p},-\mathbf{p}'}\left(\tfrac{L}{2\pi}\right)^2 \quad \forall r, s = \pm \tag{17}$$

and $\hat{J}_{r,s}(\mathbf{p})^\dagger = \hat{J}_{r,s}(-\mathbf{p})$*. Moreover,* $\hat{J}_{r,s}(\mathbf{p})\Omega = 0\ \forall \mathbf{p}$ *such that* $rp_s \geq 0$*.*

(b) The nodal Hamiltonian in (9) is identical with

$$H_n = \left(\tfrac{1}{L}\right)^2 \sum_{\mathbf{p}\in\tilde{\Lambda}^*}\sum_{r,s=\pm}\Big(\pi\tilde{a}v_F :\hat{J}_{r,s}\hat{J}_{r,s}(\mathbf{p}): + \chi(\mathbf{p})\big[g_1\hat{J}_{r,s}\hat{J}_{-r,s}(\mathbf{p}) + g_2\sum_{r'=\pm}\hat{J}_{r,s}\hat{J}_{r',-s}(\mathbf{p})\big]\Big) \tag{18}$$

and well-defined provided that $V < 4\pi t/\sin(Q)$*.*

(Proof outlined in Section 6.)

As discussed in Section 6, his theorem provides the means to exactly map H_n to a bosons Hamiltonian. Thus, the model above is equivalent to a model of non-interacting bosons coupled linearly to the antinodal fermions. It is therefore possible to integrate out the nodal fermions exactly and thus obtain an effective antinodal model. We also discuss how these results can be used to obtain physical information about the 2D t-V model.

4 Physics motivation

Our aim is to rewrite and modify the 2D t-V model such that, (i) the resulting model can be treated by bosonization, (ii) the low energy physics is changed as little as possible. For that we adopt the following hypothesis that has been successful in 1D:

H1: *There exists some underlying Fermi surface dominating the low energy physics, and we can modify, ignore or add degrees of freedom far away from this surface* (in the latter two cases we need to correct the definition of doping, of course).

We note that, at half filling and without interactions, the relevant Fermi surface is the square $|k_1 \pm k_2| = \pi/a$ (the large diamond in Figure 1). We assume that the underlying Fermi surface remains close to this square even in the presence of interactions and away from half filling. We observe that the band relation has a qualitatively different behavior in different regions of the Brillouin zone close to such a surface. To make this explicit, we select six representative points $\mathbf{Q}_{r,s}/a$ labeled by two indices $r = \pm$ and $s = 0, \pm$ as follows,

$$\begin{aligned} &\mathbf{Q}_{+,0} = (\pi, 0), \quad \mathbf{Q}_{-,0} = (0, \pi) \\ &\mathbf{Q}_{r,s} = (rQ, rsQ) \ \text{ for } r, s = \pm \end{aligned} \tag{19}$$

for some $Q \approx \pi/2$ (the dots in Figure 1). We then approximate the band relation close to these points by truncating the Taylor series at the lowest non-trivial order, $\epsilon(\mathbf{Q}_{r,s}/a + \mathbf{k}) \approx \epsilon_{r,s}(\mathbf{k})$ with

$$\epsilon_{r,0}(\mathbf{k}) = -rc_F k_+ k_-, \quad \epsilon_{r,\pm}(\mathbf{k}) = -4t\cos(Q) + rv_F k_\pm \tag{20}$$

and the constants c_F and v_F in (14). At half-filling we expect $Q = \pi/2$, and, for symmetry reasons, the underlying Fermi surface should always contain four such points $\mathbf{Q}_{r,\pm}$, $r = \pm$,

for some value of Q. Thus, the band relation is hyperbolic close to the vertices $\mathbf{Q}_{r,0}/a$ of the square surface, and it is linear with a constant Fermi velocity v_F close to the midpoints of the sides $\mathbf{Q}_{r,\pm}/a$. We use the terminology of experimental physicists studying cuprate superconductors with ARPES [23] and refer to the regions in Fourier space close to $\mathbf{Q}_{r,0}/a$ and $\mathbf{Q}_{r,\pm}/a$ as antinodal and nodal, respectively.

As will become clear in the next section, Hypothesis H1 is not enough to justify the approximations we make. For that the following somewhat stronger hypothesis is needed.

H1': *The low energy properties of the model are not (much) changed if we modify the band structure and the interactions for fermion degrees of freedom far away from the six Fermi surface points $\mathbf{Q}_{r,s}/a$ in (19).*

There are physical arguments suggesting that, at half filling and sufficiently large coupling, the 2D t-V model has a charge density wave (CDW) groundstate which is insulating; see e.g. Section IV.A in Ref. [22]. In mean fields theory this state is characterized by a CDW gap $\Delta > 0$ changing the band relations to $\pm\sqrt{\epsilon(\mathbf{k})^2 + \Delta^2}$, and this corresponds to a fully gapped underlying Fermi surface. Moreover, ARPES results on cuprate superconductors show that there exists an interesting doping regime away from half filling where, in these materials, the antinodal fermions are gapped while the nodal fermions have no gap but Fermi surface arcs [23]. This suggests that the nodal- and antinodal fermion degrees of freedom can have different physical behavior, and it motivates us to rewrite the 2D t-V model so that nodal- and antinodal fermion degrees of freedom can be easier treated by different computation methods.

The model thus obtained can be further simplified by the following hypothesis motivated by the ARPES results mentioned above.

H2: *There exists a finite doping region away from half filling where the nodal points on the underlying Fermi surface move to $\mathbf{Q}_{r,\pm}/a$ with $Q > \pi/2$, and in this regime the CDW gap is absent in the nodal regions while it is still present in the antinodal regions.*

In this regime, the parameter Q is determined by doping. This hypothesis is also suggested to us by results from renormalization group studies [24, 25] and mean field theory [26, 27].

5 Derivation of the model

We now outline a derivation of the model in (8)–(16) from the 2D t-V model, emphasizing the approximations that are made.

We divide the Brillouin zone in six regions as shown in Figure 1 (the areas enclosed by boldface lines), and we label the fermion degrees of freedom in these regions as follows,

$$\hat{\psi}_{r,s}(\mathbf{k}) = \hat{\psi}([\mathbf{Q}_{r,s}/a + \mathbf{k}]) \tag{21}$$

where the momenta $\mathbf{k}$ are now restricted to the small regions $\Lambda^*_{r,s}$ containing only momenta satisfying $-\pi/\tilde{a} \leq k_\pm < \pi/\tilde{a}$ for $s = 0$, and $-\pi/\tilde{a} \leq k_{-s} < \pi/\tilde{a}$, $-\pi/(2a) \leq k_1 + r(Q -$

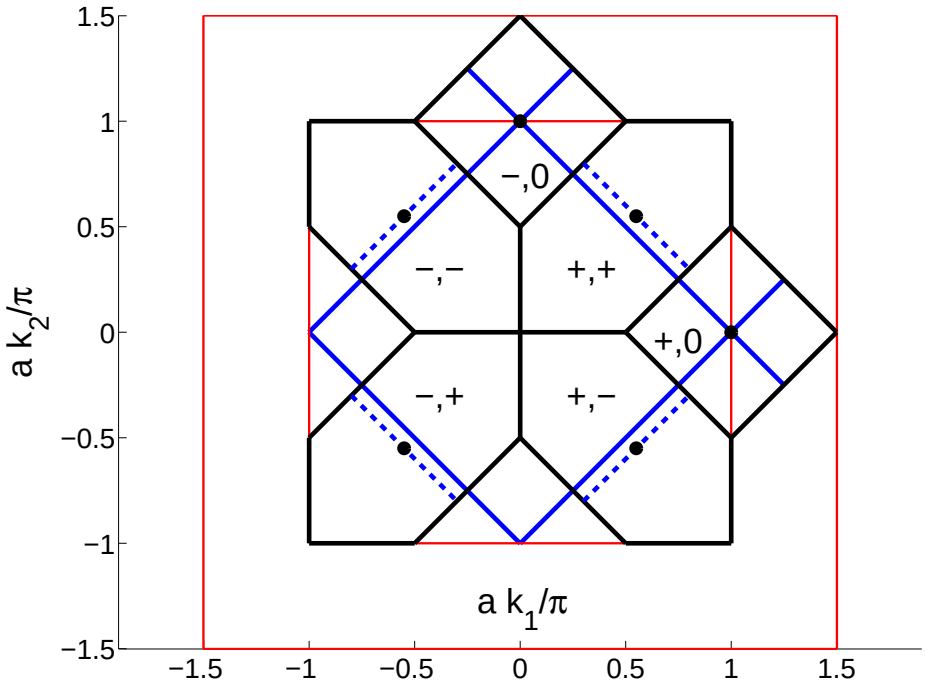

Figure 1: Division of the Brillouin zone in six regions $\Lambda^*_{r,s}$, $r = \pm$, $s = 0, \pm$. The six dots mark the points $\mathbf{Q}_{r,s}/a$ in (19) for filling $\nu = 0.55$. The regions $\Lambda^*_{r,s}$ are equal to the six-sided polygons (for $s = \pm$) and small diamonds (for $s = 0$) shifted such that the corresponding points $\mathbf{Q}_{r,s}/a$ coincide with the origin of the coordinate system. Shown are also the half-filled square surface (large diamond) and the assumed interacting Fermi surface for the nodal fermions (dashed lines).

$\pi/2)/a < \pi/(2a)$, $-\pi/(2a) \leq k_2 + rs(Q - \pi/2)/a < \pi/(2a)$ for $s = \pm$; see Figure 1. We also assume $\pi/4 < Q < 3\pi/4$ and $Q \in \sqrt{2}\pi(a/L)\mathbb{N}$ (the latter restriction becomes irrelevant in the limit $L/a \to \infty$). We thus trade different regions in the Brillouin zone for six different fermions flavors r, s. Note that $\Lambda^*_{\pm,0} = \Lambda^*_0$ in (7), and the regions are defined such that

$$\sum_{\mathbf{k}\in \mathrm{BZ}} f(\mathbf{k}) = \sum_{r,s} \sum_{\mathbf{k}\in\Lambda^*_{r,s}} f([\mathbf{Q}_{r,s}/a + \mathbf{k}]) \tag{22}$$

for any function f on BZ where, here and in the following, sums over r and s are over $r = \pm$ and $s = 0, \pm$ unless stated otherwise. In particular, $N = \sum_{r,s} N_{r,s}$ with

$$N_{r,s} = \left(\tfrac{2\pi}{L}\right)^2 \sum_{\mathbf{k}\in\Lambda^*_{r,s}} \hat{\psi}^\dagger_{r,s}\hat{\psi}_{r,s}(\mathbf{k}) \tag{23}$$

and $H_0 = \sum_{r,s}(2\pi/L)^2 \sum_{\mathbf{k}\in\Lambda^*_{r,s}} \epsilon(\mathbf{Q}_{r,s}/a + \mathbf{k})\hat{\psi}^\dagger_{r,s}\hat{\psi}_{r,s}(\mathbf{k})$. We now make our first approximation:

A1: *Taylor expand the exact band relations in the vicinity of the Fermi surface points* $\mathbf{Q}_{r,s}/a$ *and keep only the leading non-trivial terms, i.e. replace* $\epsilon(\mathbf{Q}_{r,s}/a+\mathbf{k})$ *in* H_0 *above by* $\epsilon_{r,s}(\mathbf{k})$ *in (20).*

We thus obtain

$$H_0 = \sum_{r,s} \left(\tfrac{2\pi}{L}\right)^2 \sum_{\mathbf{k}\in\Lambda^*_{r,s}} \epsilon_{r,s}(\mathbf{k})\, \hat{\psi}^\dagger_{r,s}\hat{\psi}_{r,s}(\mathbf{k}). \tag{24}$$

In this approximation, we neglect terms of higher order in $a\mathbf{k}$. We expect that the low energy properties of the model are dominated by states close to the Fermi surface points for which these higher order terms are negligible.

To modify the interaction part of the Hamiltonian in a way suitable for our purposes we use (22) to rewrite

$$\begin{aligned} H_{\rm int} = \left(\tfrac{2\pi}{L}\right)^6 \sum_{r,s}\sum_{\mathbf{k}_j\in\Lambda^*_{r,s}} & \hat{\psi}^\dagger_{r_1,s_1}(\mathbf{k}_1)\hat{\psi}_{r_2,s_2}(\mathbf{k}_2)\hat{\psi}^\dagger_{r_3,s_3}(\mathbf{k}_3)\hat{\psi}_{r_4,s_4}(\mathbf{k}_4)\hat{u}(\mathbf{Q}_{r_1,s_1}-\mathbf{Q}_{r_2,s_2}+\mathbf{k}_1-\mathbf{k}_2) \\ & \times\delta_a(\mathbf{Q}_{r_1,s_1}-\mathbf{Q}_{r_2,s_2}+\mathbf{Q}_{r_3,s_3}-\mathbf{Q}_{r_4,s_4}+\mathbf{k}_1-\mathbf{k}_2+\mathbf{k}_3-\mathbf{k}_4) \end{aligned} \tag{25}$$

and make our second approximation:

A2: *Replace the interaction Hamiltonian in (25) by*

$$\begin{aligned} H_{\rm int} = \left(\tfrac{2\pi}{L}\right)^6 \sum_{r,s}\sum_{\mathbf{k}_j\in\Lambda^*_{r,s}} & \hat{\psi}^\dagger_{r_1,s_1}(\mathbf{k}_1)\hat{\psi}_{r_2,s_2}(\mathbf{k}_2)\hat{\psi}^\dagger_{r_3,s_3}(\mathbf{k}_3)\hat{\psi}_{r_4,s_4}(\mathbf{k}_4)\hat{u}(\mathbf{Q}_{r_1,s_1}-\mathbf{Q}_{r_2,s_2}) \\ & \times\delta_a(\mathbf{Q}_{r_1,s_1}-\mathbf{Q}_{r_2,s_2}+\mathbf{Q}_{r_3,s_3}-\mathbf{Q}_{r_4,s_4})\delta_{\mathbf{k}_1-\mathbf{k}_2+\mathbf{k}_3-\mathbf{k}_4,\mathbf{0}}. \end{aligned} \tag{26}$$

Note that $\mathbf{Q}_{r_1,s_1}-\mathbf{Q}_{r_2,s_2}+\mathbf{Q}_{r_3,s_3}-\mathbf{Q}_{r_4,s_4}$ is either $\mathbf{0}$ or a "large" vector whose length is of order π/a. We expect that the most important processes for the low energy properties of the model are those where the $\mathbf{k}_j$ are so small that the Kronecker delta in (25) can be non-zero only if $\mathbf{k}_1-\mathbf{k}_2+\mathbf{k}_3-\mathbf{k}_4=\mathbf{0}$, and these processes are not much affected by A2.

To simplify (26) we have to find all solutions of $\delta_a(\mathbf{Q}_{r_1,s_1}-\mathbf{Q}_{r_2,s_2}+\mathbf{Q}_{r_3,s_3}-\mathbf{Q}_{r_4,s_4})=1$. We assume $Q\neq\pi/2$ and obtain after straightforward computations [19]

$$\begin{aligned} H_{\rm int} = \left(\tfrac{1}{L}\right)^2 \sum_{\mathbf{p}\in\tilde{\Lambda}^*} \big[& g_3 \sum_{r=\pm} \hat{\rho}^\dagger_{r,0}\hat{\rho}_{-r,0}(\mathbf{p}) + g_1 \sum_{r,s=\pm} \hat{\rho}^\dagger_{r,s}\hat{\rho}_{-r,s}(\mathbf{p}) \\ & + g_2 \sum_{r,r',s=\pm} \hat{\rho}^\dagger_{r,s}\hat{\rho}_{r',-s}(\mathbf{p}) + g_4 \sum_{r,r',s=\pm} \hat{\rho}^\dagger_{r,0}\hat{\rho}_{r',s}(\mathbf{p})\big] \end{aligned} \tag{27}$$

with

$$\hat{\rho}_{r,s}(\mathbf{p}) = \left(\tfrac{2\pi}{L}\right)^2 \sum_{\mathbf{k}_j\in\Lambda^*_{r,s}} \hat{\psi}^\dagger_{r,s}(\mathbf{k}_1)\hat{\psi}_{r,s}(\mathbf{k}_2)\delta_{\mathbf{k}_1+\mathbf{p},\mathbf{k}_2} \tag{28}$$

and the coupling parameters in (15).

The operators in (28) have the natural physical interpretation as Fourier transformed density operators. It is remarkable that we only get interaction terms of density-density

form. Our assumption $Q \neq \pi/2$ is important since otherwise one obtains additional terms that cannot be treated in a simple manner by bosonization, similarly as in 1D [8]. Such terms might cause a nodal fermion gap. This is consistent with our Hypothesis H2 in Section 4 since $Q = \pi/2$ corresponds to half filling, as shown below.

To obtain a model that can be bosonized we want to remove the UV cutoff for the nodal fermions orthogonal to the Fermi surface arcs. Before we can do that we have to normal order all fermion operators with respect to some suitable reference state Ω ("Dirac sea") with fixed fermion density $\nu \neq 1/2$. We choose this state such that the nodal fermion states are filled up to the Fermi surface through the points $\mathbf{Q}_{r,\pm}/a$ parallel to the half-filled one (the four dashed lines in Figure 1). For simplicity we also assume that the antinodal fermions are half-filled (one can show that this follows from our Hypothesis H2), but this is not essential (see [20] for a more general treatment). This reference state can be defined by the conditions in (13) *ff*. By simple geometric considerations we find that the contributions of the different regions r, s to the total filling ν of this state are $\nu_{r,0} = 1/16$ and $\nu_{r,s=\pm} = (Q/\pi - 1/8)/4$, respectively, and thus $\nu = \sum_{r,s} \nu_{r,s} = Q/\pi$.

Normal ordering of the Hamiltonian $H_0 - \mu N + H_{\rm int}$ amounts to the following: rewrite $H_{\rm int}$ in terms of the normal ordered fermion densities

$$\hat{J}_{r,s}(\mathbf{p}) = :\hat{\rho}_{r,s}(\mathbf{p}): \tag{29}$$

and normal order H_0 and N, dropping an irrelevant additive constant. An important consequence of this and Approximation A1 is a change of the chemical potential term $-\mu N$ in the Hamiltonian to $-\sum_{r,s} \mu_{r,s} : N_{r,s} :$, and we find by straightforward computations the following renormalized chemical potentials: $\mu_{r,0} = \mu - (2Q/\pi)V \equiv \mu_a$ and $\mu_{r,s=\pm} = \mu + 4t\cos(Q) - [2Q\sin^2(Q)/\pi + \cos^2(Q) + \cos(Q)/4]V \equiv \mu_n$. To have an underlying Fermi surface as assumed in H2 we set $\mu_n = 0$. This fixes μ and implies (16). Note that μ_a changes sign under the transformation $Q \to \pi - Q$, as required by invariance under particle-hole transformations.

By assumption the groundstate expectation values of $:N_{r,s}:$ all are zero in the parameter regime of interest to us, and thus the filling factor of the groundstate is identical with $\nu = Q/\pi$. This fixes Q as in (14).

We now can partially remove the UV cutoff for the nodal fermions. We do this by a sequence of three approximations:

A3: *Replace in the interaction part of the Hamiltonian the normal ordered nodal densities* $\hat{J}_{r,s=\pm}(\mathbf{p})$ *by* $\chi(\mathbf{p})\hat{J}_{r,s=\pm}(\mathbf{p})$ *with the cutoff functions* χ *in (12).*

A4: *Replace the nodal Fourier space regions* $\Lambda^*_{r,s=\pm}$ *by the sets* $\Lambda^*_{s=\pm}$ *in (7), i.e., drop the restriction on* k_s*.*

A5: *Replace in the interaction part of the Hamiltonian the normal ordered nodal fermion densities*

$$\hat{J}_{r,s=\pm}(\mathbf{p}) = \left(\tfrac{2\pi}{L}\right)^2 \sum_{\mathbf{k}\in\Lambda^*_s} :\hat{\psi}^\dagger_{r,s}(\mathbf{k}-\mathbf{p})\hat{\psi}_{r,s}(\mathbf{k}): \tag{30}$$

by the ones in (11), i.e. add the umklapp terms $n \neq 0$ *parallel to the Fermi surface arc.*

We thus obtain the model in (8)–(16).

Note that in approximations A4 and A5 we add terms to the nodal fermion densities, and we therefore increase the number of interaction terms in the Hamiltonian. Approximation A2 partly compensates for this. To be more specific: before A3, the number of terms included in the nodal fermion density $J_{r,s=\pm}(\mathbf{p})$ decreases linearly with $|p_+|$ and $|p_-|$ until $|p_\pm| = 2\pi/\tilde{a}$ when it becomes zero. However, after A4 and A5 this number of terms becomes infinite and independent of $\mathbf{p}$. It therefore is natural to restrict the interaction terms involving nodal fermions densities by imposing a cutoff on $\mathbf{p}$. We do not know a physical argument that fixes this cutoff in a unique manner. However, we believe that the properties of the model are not sensitive to changes of this cutoff. We therefore choose here a cutoff that is particularly simple; see [19] for a more general treatment.

Our arguments above can be generalized to lattice models with more general band relations, and our choice for the regions Λ_s^* can be generalized by introducing an additional parameter allowing to change the widths of the nodal regions $\Lambda_\pm^*$ [19]. Moreover, it is not necessary to use the simplified band relations $\epsilon_{r,0}$ and interaction vertices for the antinodal fermions, and we only do this here for aesthetic reasons. It also is possible to relax Hypothesis H2 [20], as already mentioned.

It would be interesting to check in more detail if the approximations above indeed do not change the low energy properties of the model. This can be done, in principle, using our results: one can bosonize also the terms that we added or dropped in our approximations, and one should be able investigate the effect of these terms on the groundstate using renormalization group methods. This is an interesting project for the future.

6 Bosonization and partial exact solution

The arguments in this section can be made mathematically precise [19, 21].

We first outline a proof of the theorem in Section 3. For that it is useful to formally write the model in (9)–(11) in position space as follows (we suppress arguments $\mathbf{x}$ below),

$$H_n = \int \mathrm{d}^2x \sum_{s=\pm} :\Big(\sum_r r v_F\, \psi^\dagger_{r,s}(-\mathrm{i}\partial_s)\psi_{r,s} + g_1 \sum_r J_{r,s}J_{-r,s} + g_2 \sum_{r,r'} J_{r,s}J_{r',-s}\Big): \qquad (31)$$

for the nodal part ($\partial_\pm$ means $\partial/\partial x_\pm$), and

$$H_a = \int \mathrm{d}^2x :\Big(\sum_r \psi^\dagger_{r,0}(r c_F \partial_+\partial_- - \mu_a)\psi_{r,0} + g_3 \sum_r J_{r,0}J_{-r,0} + g_4 \sum_{s=\pm,r,r'} J_{r,0}J_{r',s}\Big): \qquad (32)$$

for the antinodal including the mixed parts, with $J_{r,s}(\mathbf{x}) =: \psi^\dagger_{r,s}(\mathbf{x})\psi_{r,s}(\mathbf{x}) :$ the normal ordered fermion densities. The proper interpretation of these formulas follows from the precise definition of the model in Fourier space: different fermion flavors $\psi_{r,s}$ come with different Fourier space regions Λ_s^*, and thus the spatial variable $\mathbf{x}$ in

$$\psi_{r,s}(\mathbf{x}) = (\tfrac{2\pi}{L})^2 \sum_{\mathbf{k}\in\Lambda_s^*} \hat{\psi}_{r,s}(\mathbf{k}) \exp(\mathrm{i}\mathbf{k}\cdot\mathbf{x}) \qquad (33)$$

lives on different spaces: for the fermions $\psi_{r,+}(\mathbf{x})$ only the variable x_+ is continuous while x_- lives on a 1D lattice with lattice constant $\tilde{a}$ and length L, and similarly for $\psi_{r,-}(\mathbf{x})$ with x_+ and x_- interchanged (note that the umklapp terms with $n \neq 0$ in (11) are needed for this interpretation to be consistent with Fourier transformation). Thus the integrals here should be (partly) interpreted as Riemann sums [19]. In particle physics parlance, $1/\tilde{a}$ is a UV cutoff needed to give a precise mathematical meaning to the model.

Thus $\psi_{r,+}(\mathbf{x})$ in (31) can be treated as a collection of 1D Dirac fermions where x_+ plays the role of the 1D space coordinate and x_- of a flavor index. We therefore can use the standard mathematical results of 1D bosonization; see e.g. [9] or [10]. These imply that the densities $J_{r,+}$ obey the following commutator relations,

$$[J_{r,+}(\mathbf{x}), J_{r',+}(\mathbf{y})] = \delta_{r,r'} r \frac{1}{2\pi \mathrm{i}\tilde{a}} \partial_+ \delta^2(\mathbf{x}-\mathbf{y}) \tag{34}$$

where $\delta^2(\mathbf{x}-\mathbf{y})$ here means $\delta(x_+ - y_+)\delta_{x_-,y_-}/\tilde{a}$, and

$$r \int \mathrm{d}^2x \; :\psi^\dagger_{r,+}(-\mathrm{i}\partial_+)\psi_{r,+}: = \tilde{a} \int \mathrm{d}^2x \; :J^2_{r,+}: \tag{35}$$

where $\int \mathrm{d}^2x$ stands for $\int \mathrm{d}x_+ \sum_{x_-} \tilde{a}$. These and similar formulas for $\psi_{r,-}$ imply (17) and (18). The other relations stated in part (a) of the theorem in Section 3 follow from well-known corresponding results in 1D.

We now describe how to exactly diagonalize the bosonized nodal Hamiltonian H_n. For simplicity we continue our discussion in position space and ignore UV cutoffs that do not affect the results we mention (a more detailed solution, including all cutoffs explicitly, can be found in [19]). The commutator relations in (34) imply that the operators

$$\begin{aligned} \partial_\pm \Phi_\pm &= \sqrt{\pi\tilde{a}}\,(J_{+,\pm} + J_{-,\pm}) \\ \Pi_\pm &= \sqrt{\pi\tilde{a}}\,(-J_{+,\pm} + J_{-,\pm}) \end{aligned} \tag{36}$$

obey the commutator relations of standard 2D boson fields: $[\Phi_\pm(\mathbf{x}), \Pi_\pm(\mathbf{y})] = \mathrm{i}\delta^2(\mathbf{x}-\mathbf{y})$ etc., and by straightforward computations one finds that the nodal Hamiltonian can be expressed in terms of these bosons as follows,

$$H_n = \frac{v_F}{2} \int \mathrm{d}^2x : \Big(\sum_{s=\pm} [(1-\gamma)\Pi_s^2 + (1+\gamma)(\partial_s \Phi_s)^2] + 2\gamma(\partial_+\Phi_+)(\partial_-\Phi_-) \Big) : \tag{37}$$

where $\gamma = V \sin(Q)/(4\pi t)$. It is important to note that this Hamiltonian is positive definite only if $\gamma < 1$, and this implies an upper bound on the interaction strength mentioned in the theorem in Section 3, similarly as in 1D. Fortunately, this bound is satisfied for interesting parameter values (V/t from 0 up to 12 or so).

We thus obtain an exact representation of the 2D analogue of the Luttinger model as a system of non-interacting bosons coupled linearly to the interacting antinodal fermions. The boson Hamiltonian in (37) can be diagonalized by standard methods, and we find

$$H_n = \mathcal{E}_n + \left(\tfrac{2\pi}{L}\right)^2 \sum_{\mathbf{p}} \sum_{s=\pm} \omega_s(\mathbf{p}) b^\dagger_s(\mathbf{p}) b_s(\mathbf{p}) \tag{38}$$

with some computable constant $\mathcal{E}_n$, the dispersion relations

$$\omega_{\pm}(\mathbf{p}) = \frac{v_F}{2\sqrt{2}}\sqrt{1-\gamma^2}\sqrt{|\mathbf{p}|^2 \pm \sqrt{|\mathbf{p}|^4 - (1-[\gamma/(1+\gamma)]^2)(2p_+p_-)^2}}, \tag{39}$$

and standard boson operators $b_s(\mathbf{p})$, i.e $[b_{\pm}(\mathbf{p}), b^{\dagger}_{\pm}(\mathbf{p}')] = \delta^2(\mathbf{p}-\mathbf{p}')$ etc. Note that the anisotropy of the non-interacting systems is reduced by $\gamma \neq 0$. Using that it is straightforward to compute the exact energy eigenstates, energy eigenvalues, and partition function for the model defined by the Hamiltonian in (9).

One can also exactly integrate out the bosons and thus derive an effective action for the antinodal fermions. We found that, in a good approximation, this action can be represented by an effective Hamiltonian that has the same form as H_a in (10) but with the coupling constants changed to [19]

$$g_3 = 2Va^2\left(1 - \frac{V}{2\sin(Q)[2\pi t + V\sin(Q)]}\right), \quad g_4 = 0. \tag{40}$$

It is possible to compute the CDW gap $\Delta \propto \langle \psi^{\dagger}_{+,0}\psi_{-,0}\rangle$ for this latter effective antinodal model using mean field theory [20]. We found that $\langle :N_a: \rangle = \langle :N_n: \rangle = 0$ and $\Delta > 0$ are indeed independent of the parameter μ_a for intermediate values of V/t and in some Q-interval around $Q = \pi/2$ [20], in agreement with Hypothesis H2 in Section 4 .

We believe that, after bosonization, it is possible to make mathematical sense of the continuum limit $\tilde{a} \to 0$ of the nodal Hamiltonian, but we expect that this requires non-trivial additive and multiplicative renormalizations, similarly as in 1D [28]. This would give further support to our conjecture that the approximations in Section 5 do not affect the low energy properties of the model.

7 Final remarks

We argued that there exists a parameter regime away from half filling where the antinodal fermions $\psi_{r,0}$ are gapped. We propose that, in this regime, the nodal Hamiltonian in (9) alone accounts for the low energy physics of the 2D t-V model. This nodal model is exactly solvable by bosonization and, in particular, it is possible to compute all its Green's function by analytical methods. It would be interesting to do this and thus confront this model with experimental results on 2D correlated fermion systems. We hope to come back to this in the near future [21].

While the 2D analogue of the Luttinger model becomes particular simple in the regime where the antinodal fermions are gapped, it can be used also for other parameter values [20]. We believe that a mean field treatment of the antinodal fermions is appropriate to compute phase diagrams. However, in parameter regions where mean field theory predicts that the antinodal fermions are gapless, a treatment of the antinodal Hamiltonian in (10) beyond mean field theory would be desirable.

Our approach can be straightforwardly generalized to 2D lattice fermion models with more complicated band relations [19, 20] and spin [21], similarly as in 1D [8].

It is known that the truncated nodal model in (9) with $g_2 = 0$ has "Luttinger liquid" behavior after [29] but not before Approximation A5 [30]. However, we believe that our model with $g_2 > 0$ is less sensitive to Approximation A5 than the truncated model with $g_2 = 0$. The reason is that the boson propagator has better decaying properties in Fourier space for $g_2 > 0$ than for $g_2 = 0$ (since the boson dispersion relations in (39) are quite isotropic, whereas for $g_2 = 0$ they are $\omega_\pm(\mathbf{p}) \propto |p_\pm|$ independent of $p_\mp$).

Although we suggest that the model in (8)–(11) is a 2D analogue of the Luttinger model, we emphasize that we do *not* state that this model has "Luttinger-liquid" behavior [15]: if or not this is the case is a delicate question and remains to be seen. We plan to come back to this in the near future [21].

We finally discuss previous work related to ours. The pioneer in higher dimensional bosonization is Luther [11]. To our knowledge it was Mattis [12] who first made the important observation that a 2D model similar to our nodal fermion model (i.e. no antinodal fermions) is exactly solvable by bosonization; see also Ref. [13, 14] for previous work on Mattis' model. Our work can be regarded as a particular implementation of the idea promoted by Anderson [15] that 2D interacting fermions systems can be understood by bosonization in each direction of some Fermi surface. An earlier implementation of this idea and starting with a square Fermi surface is by Luther [16], but different from him we bosonize chains in position space (rather than Fourier space) and thus can avoid certain approximations in the treatment of the interactions. Various other implementations of the idea to bosonize 2D fermion systems appeared in the literature before but seem to differ in detail from ours; see e.g. [17, 18] and references therein. We finally mention other work that was important as inspiration for us, namely renormalization group studies of the 2D Hubbard model [24, 25] and work by Schulz [26] emphasizing the significance of the antinodal fermions for 2D lattice fermion systems.

Acknowledgments. I acknowledge helpful discussions with Alexios Polychronakos, Asle Sudbø, Manfred Salmhofer and Mats Wallin. I also would like to thank anonymous referees, Vieri Mastropietro, and in particular Jonas de Woul for constructive criticism that helped me to improve this paper. This work was supported by the Swedish Science Research Council (VR), the Göran Gustafsson Foundation, and the European Union through the FP6 Marie Curie RTN *ENIGMA* (Contract number MRTN-CT-2004-5652).

References

[1] J. M. Luttinger: An exactly soluble model of a many-fermion system, J. Math. Phys. **4**, 1154 (1963)

[2] D. C. Mattis and E. H. Lieb: Exact solution of a many-fermion system and its associated boson field, J. Math. Phys. **6**, 304 (1965)

[3] S. Tomonaga: Remarks on Bloch's method of sound waves applied to many-fermion problems, Prog. Theor. Phys. **5**, 544 (1950)

[4] W. Thirring: A soluble relativistic field theory, Ann. Phys. **3**, 91 (1958)

[5] K. Johnson: Solution of the equations for the Green functions of a two dimensional relativistic field theory, Nuovo Cim. **20**, 773 (1961)

[6] R. Heidenreich, R. Seiler, D. A. Uhlenbrock: The Luttinger model, J. Stat. Phys. **22**, 27 (1980)

[7] F. D. M. Haldane: "Luttinger liquid theory" of one-dimensional quantum fluids: I. Properties of the Luttinger model and their extension to the general 1D interacting spinless Fermi gas, J. Phys. C **14**, 2585 (1981)

[8] A. O. Gogolin, A. A. Nersesyan, and A. M. Tsvelik: Bosonization and strongly correlated systems. Cambridge University Press, Cambridge (1998)

[9] See e.g.: A.L. Carey and S.N.M. Ruijsenaars: On fermion gauge groups, current algebras and Kac-Moody algebras, Acta Appl. Mat. **10**, 1 (1987)

[10] J. von Delft and H. Schoeller: Bosonization for beginners - refermionization for experts, Ann. Phys. (Leipzig) **7**, 225 (1998)

[11] A. Luther: Tomonaga fermions and the Dirac equation in three dimensions, Phys. Rev. B **19**, 320 (1979)

[12] D. C. Mattis: Implications of infrared instability in a two-dimensional electron gas, Phys. Rev. B **36**, 745 (1987)

[13] D. V. Khveshchenko, R. Hlubina and T. M. Rice: Non-Fermi-liquid behavior in two dimensions due to long-ranged current-current interactions, Phys. Rev. B **48**, 10766 (1993)

[14] R. Hlubina: Luttinger liquid in a solvable two-dimensional model, Phys. Rev. B **50**, 8252 (1994)

[15] P. W. Anderson: "Luttinger-liquid" behavior of the normal metallic state of the 2D Hubbard model, Phys. Rev. Lett. **64**, 1839 (1990)

[16] A. Luther: Interacting electrons on a square Fermi surface, Phys. Rev. B **50**, 11446 (1994)

[17] A. Houghton, H.-J. Kwon, J. B. Marston: Multidimensional bosonization, Adv. Phys. **49**, 141 (2000) [`cond-mat/9810388`]

[18] A. P. Polychronakos: Bosonization in higher dimensions via noncommutative field theory, Phys. Rev. Lett. **96**, 186401 (2006)

[19] E. Langmann: A 2D Luttinger model, `arXiv:0903.0055v3 [math-ph]`

[20] J. de Woul and E. Langmann: Partially gapped fermions in 2D, J. Stat. Phys. (to appear) `arXiv:0907.1277v2 [math-ph]`

[21] J. de Woul and E. Langmann (work in progress)

[22] R. Shankar: Renormalization-group approach to interacting fermions, Rev. Mod. Phys. **66**, 129 (1994)

[23] For review see e.g. A. Damescelli, Z. Hussain and Z.-X. Shen: Angle-resolved photoemission studies of the cuprate superconductors, Rev. Mod. Phys. **75**, 473 (2003)

[24] N. Furukawa, T. M. Rice, and M. Salmhofer: Truncation of a two-dimensional Fermi surface due to quasiparticle gap formation at the saddle points, Phys. Rev. Lett. **81**, 3195 (1998)

[25] C. Honerkamp, M. Salmhofer, N. Furukawa, and T. M. Rice: Breakdown of the Landau-Fermi liquid in two dimensions due to umklapp scattering, Phys. Rev. B **63**, 035109 (2001)

[26] H. J. Schulz: Fermi-surface instabilities of a generalized two-dimensional Hubbard model, Phys. Rev. **39**, 2940 (1989)

[27] E. Langmann and M. Wallin: Mean field magnetic phase diagrams for the two dimensional t-t'-U Hubbard model, J. Stat. Phys. **127**, 825 (2007)

[28] H. Grosse, E. Langmann and E. Raschhofer: On the Luttinger-Schwinger model, Annals of Phys. (N.Y.) **253**, 310 (1997)

[29] V. Mastropietro: Luttinger liquid fixed point for a two-dimensional flat Fermi surface, Phys. Rev. B **77**, 195106 (2008)

[30] A. T. Zheleznyak, V. M. Yakovenko and I. E. Dzyaloshinskii: Parquet solution for a flat Fermi surface, Phys. Rev. B **55**, 3200 (1997)